Resource

Cell Reports

Lipid Cooperativity as a General Membrane-Recruitment Principle for PH Domains

Graphical Abstract

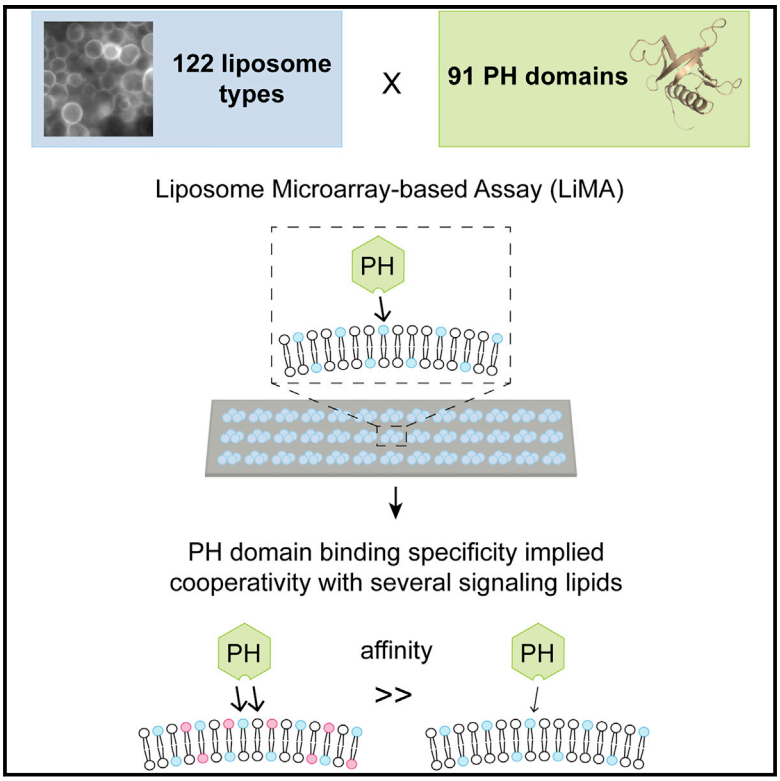

Authors

Ivana Vonkova, Antoine-Emmanuel Saliba, Samy Deghou, ..., Jan Ellenberg, Peer Bork, Anne-Claude Gavin

Correspondence

bork@embl.de (P.B.),
gavin@embl.de (A.-C.G.)

In Brief

Vonkova et al. systematically quantify the lipid-binding properties of 91 pleckstrin homology (PH) domains using a physiological, quantitative, liposome microarray-based assay. The data set reveals that cooperativity between lipids is a key mechanism for membrane recruitment of PH domains.

Highlights

- The lipid-binding properties of 91 pleckstrin homology domains have been quantified
- Over 10,000 individual protein-lipid interaction experiments have been performed
- The binding specificity and affinity imply cooperativity between signaling lipids
- Mutations found in cancer biopsies fine-tune lipid-binding specificities

Vonkova et al., 2015, Cell Reports *12*, 1519–1530
September 1, 2015
http://dx.doi.org/10.1016/j.celrep.2015.07.054

CellPress

Cell Reports
Resource

Lipid Cooperativity as a General Membrane-Recruitment Principle for PH Domains

Ivana Vonkova,[1,7] Antoine-Emmanuel Saliba,[1,2,5,7] Samy Deghou,[1,7] Kanchan Anand,[1] Stefano Ceschia,[1] Tobias Doerks,[1] Augustinus Galih,[1] Karl G. Kugler,[1] Kenji Maeda,[1] Vladimir Rybin,[3] Vera van Noort,[1,6] Jan Ellenberg,[2] Peer Bork,[1,4,*] and Anne-Claude Gavin[1,4,*]

[1]Structural and Computational Biology Unit, European Molecular Biology Laboratory (EMBL), Meyerhofstrasse 1, 69117 Heidelberg, Germany
[2]Cell Biology and Biophysics Unit, EMBL, Meyerhofstrasse 1, 69117 Heidelberg, Germany
[3]Protein Expression and Purification Core Facility, EMBL, Meyerhofstrasse 1, 69117 Heidelberg, Germany
[4]Molecular Medicine Partnership Unit, EMBL, Meyerhofstrasse 1, 69117 Heidelberg, Germany
[5]Present address: Institute for Molecular Infection Biology, University of Würzburg, Josef-Schneider-Straße 2, 97080 Würzburg, Germany
[6]Present address: KU Leuven, Centre of Microbial and Plant Genetics, Kasteelpark Arenberg 22, 3001 Leuven, Belgium
[7]Co-first author
*Correspondence: bork@embl.de (P.B.), gavin@embl.de (A.-C.G.)
http://dx.doi.org/10.1016/j.celrep.2015.07.054

SUMMARY

Many cellular processes involve the recruitment of proteins to specific membranes, which are decorated with distinctive lipids that act as docking sites. The phosphoinositides form signaling hubs, and we examine mechanisms underlying recruitment. We applied a physiological, quantitative, liposome microarray-based assay to measure the membrane-binding properties of 91 pleckstrin homology (PH) domains, the most common phosphoinositide-binding target. 10,514 experiments quantified the role of phosphoinositides in membrane recruitment. For most domains examined, the observed binding specificity implied cooperativity with additional signaling lipids. Analyses of PH domains with similar lipid-binding profiles identified a conserved motif, mutations in which—including some found in human cancers—induced discrete changes in binding affinities in vitro and protein mislocalization in vivo. The data set reveals cooperativity as a key mechanism for membrane recruitment and, by enabling the interpretation of disease-associated mutations, suggests avenues for the design of small molecules targeting PH domains.

INTRODUCTION

A eukaryotic cell usually produces more than 1,000 different lipid species that possess a wide range of structural, physical, and biochemical properties. These lipids have a role in virtually all biological processes (van Meer, 2005) through their extensive, regulated association with other lipids and proteins. The significance of these regulatory circuits is evident from the variety of human disorders arising from altered protein-lipid interactions (Bayascas et al., 2008; Lindhurst et al., 2011; Züchner et al., 2005; Köberlin et al., 2015), which constitute attractive targets for pharmaceutical drug development (Hussein et al., 2013).

Protein-lipid interactions can drive the recruitment of peripheral membrane proteins to specific subcellular membranes and thereby contribute to the organization of many cellular functions. This process involves a group of specialized lipid-binding domains (LBDs) that recognize distinctive membrane features, such as specific lipid species or head groups and membrane curvature or charge (Lemmon, 2008). For example, the seven phosphoinositide species—produced by the reversible phosphorylation of the inositol head group of phosphatidylinositol (PI)—are enriched in distinct organelles (Kutateladze, 2010). They form a molecular signature that defines the different subcellular membranes and which is read by a subgroup of LBDs, namely the phosphoinositide-binding domains (Lemmon, 2003). However, many phosphoinositide-binding domains have remarkably low affinity and specificity—if at all—for individual phosphoinositide species (Dowler et al., 2000; Lemmon, 2008; Yu and Lemmon, 2001; Yu et al., 2004). Their efficient and specific recruitment to subcellular membranes sometimes even occurs by a coincidence-sensing mechanism, implying that cooperative associations with membrane proteins and/or additional signaling lipids such as phosphatidylserine, phosphatidic acid, and sphingolipids may play a role (Anand et al., 2012; Di Paolo and De Camilli, 2006; Gallego et al., 2010; Moravcevic et al., 2012; Burger et al., 2000; Huang et al., 2011; Knight and Falke, 2009; Kutateladze et al., 2004; Lee and Bell, 1991; Lucas and Cho, 2011; Macia et al., 2000; Stahelin et al., 2003, 2004; Ziemba and Falke, 2013). However, only a few studies have so far explored this phenomenon, and a global and unbiased understanding of membrane-recruitment principles—i.e., the elusive "phosphoinositide code"—is yet to be achieved.

We therefore systematically studied the mechanisms underlying membrane recruitment in a prototypic family of phosphoinositide-binding domains—the pleckstrin homology (PH) domain, which is the most common membrane-targeting motif in eukaryotes. We have developed an approach termed a liposome

microarray-based assay (LiMA) (Saliba et al., 2014) to quantitatively profile the recruitment of 91 PH domains to a large variety of surrogate cellular membranes composed of the main classes of signaling lipids and their systematic combinations. The resulting data represent one of the largest sets of physically quantified protein-lipid interactions to date (data available at http://vm-lux.embl.de/~deghou/data/ph-domain/). They reveal some of the basic features that enable PH domains to specifically recognize membranes: that is, the selective recognition of individual phosphoinositide species and the frequent, context-specific tuning mechanisms driven by the presence of additional lipids such as phosphorylated sphingoid long-chain bases (LCBs) and phosphatidylserine, for which rheostasis might represent an important mode of action, contributing to the effective spatiotemporal fine-tuning of cell signaling.

RESULTS

Analysis of Membrane-Recruitment Mechanisms for 91 PH Yeast Domains Using LiMA

We recently developed LiMA, a method that integrates biochemical principles—that is, the assembly of surrogate of biological membranes on a thin agarose layer—with quantitative fluorescence microscopy-based imaging and microfluidics (Saliba et al., 2014). LiMA measures protein recruitment to membranes in a quantitative and multiplexed manner and is thus well suited for charting cooperative binding mechanisms on a large scale. This miniaturized array was further developed to accommodate 122 different types of liposomes, each comprising 26 different signaling lipids present in different combinations and concentrations (Figure 1A; Table S1) in assay buffer (10 mM HEPES [pH 7.5] and 150 mM NaCl) containing no phosphate that could act as competitor of the interactions (see the Supplemental Experimental Procedures). For comparison, we also included seven non-physiological analogs that are synthesized in higher eukaryotes, but not in yeast (Table S1A). These non-physiological lipids in yeast represent interesting controls to assess LBDs binding specificity and can be used as chemical analogs, which means they are included in the final data set—albeit flagged as such—but to avoid confusion, they are not included in the final analysis. As controls, liposomes carrying biotinylated phosphatidylethanolamine (PE) were placed at ten specific positions on the array, and binding to streptavidin-AF488—spiked in each cell extract—served as a general indicator for the quality of the assay (Figure S1A). The different lipid mixtures of phosphoinositide phosphates (PIPs) and other signaling lipids were chosen based on the few examples from the literature demonstrating cooperative-binding mechanisms for a limited number of LBDs (Gallego et al., 2010; Moravcevic et al., 2012; implying both PIPs and glycerophospholipid and PIPs and sphingolipids). Given the paucity of data on the exact local organization and concentration of signaling lipids in membranes in vivo (van den Bogaart et al., 2011), we opted for standard concentrations (5–10 mol %) that have been used for in vitro studies and that represent an approximation of the in vivo situation (Tables S1B and S1C). For example, PS (phosphatidylserine), PA (phosphatidic acid), PE (phosphatidylethanolamine), and PI (phosphatidylinositol) are abundant lipids, and each account for ~10 mol % of the whole-cell lipidome. This is in contrast to PIPs and sphingolipids, in which overall averaged cellular abundance is generally very low (<<1 mol %). However, these lipids are very rarely homogenously distributed inside the cell, and they are known to cluster in nano- or microdomains where their local concentration reaches very high levels (up to 80 mol % for $PI(4,5)P_2$; Table S1B; van den Bogaart et al., 2011; Trajkovic et al., 2008).

We assayed the membrane-binding properties of large number of known and predicted PH and PH-like domains in *Saccharomyces cerevisiae* (58 PH domains from 49 proteins) and their orthologs in a thermophilic fungus, *Chaetomium thermophilum* (Amlacher et al., 2011; 27 PH domains from 24 proteins). We also selected six mammalian PH domains and, for comparison, four unrelated LBDs with known and distinct lipid-binding specificities (Figure 1A; Table S2). The 95 domains were successfully produced in *Escherichia coli* as superfolder GFP (sfGFP)-tagged fusions (see the Supplemental Experimental Procedures), and their recruitment to the different liposomal membranes was measured by automated high-throughput fluorescence microscopy. To further assess the quality of the recombinant expression systems, 11 PH domains were further analyzed by circular dichroism (CD) spectroscopy, including thermal denaturation experiments (Figures S1B and S1C). The resulting data indicate that all domains were folded and stable under our experimental conditions. We processed a total of 229,880 images that were visually inspected, and experiments that were unsuccessful—for example, because of protein precipitation or a failure to produce liposomes or to acquire focused images—were removed from the data. We did not observe multilamellar vesicles or broken liposomes. All images are available to download (http://vm-lux.embl.de/~deghou/data/ph-domain/). The final data set consists of 10,514 unique protein-liposome experiments (92.3% of those designed), comprising 23,069 replicates (i.e., an average of 2.7 replicates per protein-liposome pair), in which the location of the different types of liposome on the arrays was randomly shuffled to control for any possible position bias (Figures 1A and S1A; Supplemental Experimental Procedures). For each protein-liposome experiment, we calculated a normalized binding intensity (NBI) that reflects the number of sfGFP-tagged proteins bound per membrane surface area (Saliba et al., 2014) (Table S3).

Data Quality and Reproducibility

To define binding events, we used manually inspected and annotated images to determine the parameters that gave maximum precision (i.e., the highest number of true interactions). The best conditions (NBI $\geq$ 0.037) in terms of sensitivity (75.2%) and specificity (96.6%) produced a set of 2,269 PH domain-liposome interactions (Figure S1D; Table S3). The overall (experimental and computational) reproducibility was 91.2% for distinguishing between interacting and non-interacting LBD-liposome pairs, measured on the set of 8,148 experiments for which replicates were available (Pearson correlation = 0.67; 87% of the replicates are within a two-log NBI difference; Figures 1B and S1E).

We developed a scoring system that we refer to as the "reproducibility index" (RI) to assess the confidence and reproducibility of an interaction (see the Supplemental Experimental Procedures). The RIs take into consideration not only the mean NBI

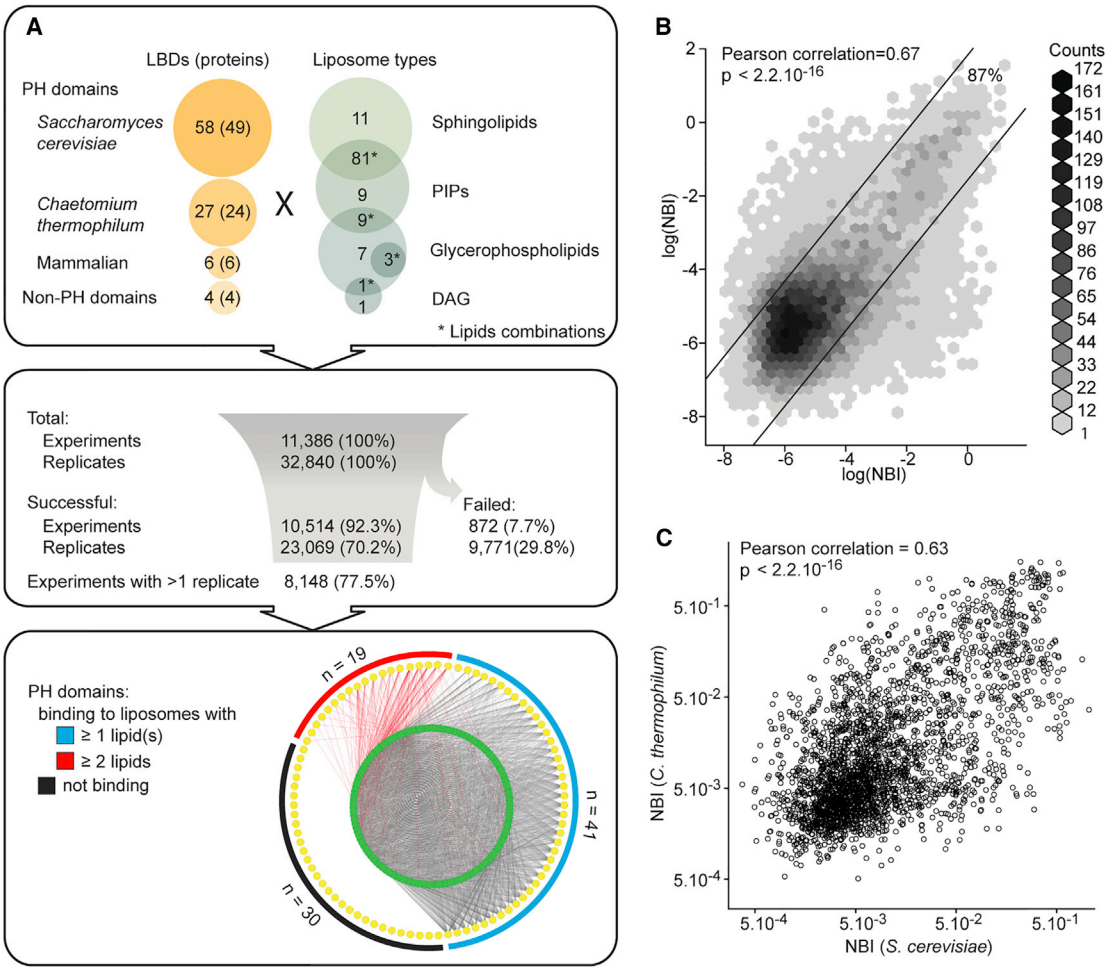

Figure 1. Overview of the PH Domain-Membrane Interactome

(A) Upper panel: selection of lipid-binding domains (LBDs, number of source proteins in parenthesis) and liposomes covered in the study. Middle panel: summary of experimental success rate is shown. Lower panel: summary of PH domain-liposome interactions detected is shown. Inner circles are liposomes, outer circles are PH domains, and lines represent high-confidence binding events.

(B) Quantitative reproducibility of the screen. The Pearson correlation of NBI values is measured for all corresponding replicates for each LBD-liposome experiment. Counts represent the number of measurements per each hexagon in the matrix. The lines delimit the replicates within two logs of difference (87%).

(C) Correlation of lipid-binding profiles of 27 pairs of orthologous PH domains from *S. cerevisiae* and *C. thermophilum*. The Pearson correlation of all corresponding normalized binding intensity (NBI) values measured for all orthologous PH domains.

See also Figure S1.

values and the NBI threshold (NBI = 0.037) but also the SE between the replicates (Figure S1F; Table S3). Reproducible binding events have low RI values. We defined a set of 1,628 high-quality PH domain-liposome interactions with a RI < 2.0.

Next, we evaluated the quality of the data set by inspecting a group of 45 PH domains in our selection that have previously been studied (Table S4). Of this set, 28 bound to at least one liposome in our assay, but four of these had not previously been seen to interact with lipids. We thus estimate our false-positive rate to be 14% (4/28). This is probably an upper limit, as among the four false positives, only one completely lacks the basic sequence motif (BSM) KXn(K/R)XR believed to be required for lipids binding (Isakoff et al., 1998; Moravcevic et al., 2012; Park et al., 2008; Yu et al., 2004) (Table S5A). The data set also recapitulates the expected specificities for the positive controls: HSV2 bound to $PI(3,5)P_2$ and PI(3)P; EEA1 and p40phox to PI(3)P; and the C2 domain of lactadherin to PS (Figure S1G). For example, the average NBIs for EEA1 and p40phox for PI(3)P-containing liposomes is approximately five times higher than for $PI(3,4)P_2$-, $PI(3,5)P_2$-, $PI(4,5)P_2$-, and $PI(3,4,5)P_3$-containing liposomes (p values from 2.4×10^{-11} to 9.8×10^{-13}; Figure S1H). We also observed that the non-physiological lipids in yeast—i.e., those synthesized in higher eukaryotes only (Table S1A)—generally bind to yeast domains in a similar manner as their natural counterparts and thus can be considered as analogs (data not shown). For example, many yeast PH domains bound to $PI(3,4,5)P_3$, which is a non-physiological lipid in this organism. It has been proposed that yeast PH domains can have broad

specificity and that PI(3,4,5)P_3-specific PH domains evolved only in more-complex species (Mitra et al., 2004).

We next assessed the sensitivity of our assay and defined a lower limit of detection by comparing the Kd values of interacting LBD-lipid pairs present in our analyses with those reported in the literature (Table S4B). Most interactions in the mid-micromolar range were successfully captured by LiMA, thus establishing a detection limit threshold. For six PH domain-liposome pairs, we produced additional dose-response experiments (increasing the PH-domain concentrations; Figure S1I). We could measure Kds ranging from 1.4 to 3.5 μM, and these were generally in agreement with previously published data. For the AKT1, PLCD1, Dynamin1, SWH1, and OSH2 PH domains that bind to different PIPs—and for which Kds are available in the literature (ranging from 0.2 to 20.7 μM)—our NBI measurement correlates well with the Kds (Figure S1J; Table S4B), indicating that our approach is sensitive and quantitative.

We also wanted to identify any potential source of bias in our results such as the experimental time needed to measure the arrays (~3 hr). To assess whether this has an effect on the data, we took advantage of the fact that we reshuffled all the lipid positions between the replicates. We did not observe a significant correlation between the NBIs measured and the time delay in the imaging (Figure S1K). We also imaged the same liposome array twice—once at time 0 and then 2 hr later—and there were no significant changes between the two sets of NBIs (Figure S1L). The large differences in the levels of expression of the 95 individual sfGFP-tagged fusions—ranging from 0.1 μM to 98 μM—might also influence the data, but we found that the expression levels did not correlate with NBIs (Figure S1M). We also considered the set of experiments for which replicates were available (Table S3) and in which the same GFP fusions were often expressed (and probed) at different concentrations (i.e., varied by more than 1.5-fold; 42 LBDs). For the majority of these 42 LBDs (88.1%), substantial changes in their concentration did not significantly affect the measured NBIs (Figure S1N; Table S2). This indicates that proteins were frequently present in the assay at saturating concentrations. In this experimental design, high variability in the binding intensity (NBIs) of different LBDs to the same liposome indicates that they have a different mode of interaction or that the number of binding sites on the liposome varies. By contrast, detailed dose-response (Kd determination) experiments are required to compare and rank LBDs recruited with similar NBIs to the same liposome.

The PH Domain-Membrane Interactome

The majority of the PH domains tested (60; 66.7%) bound efficiently (NBIs > 0.037) to at least one of the 122 different types of liposomes with high confidence (RI < 2). For 41 of them, the presence of a single phosphoinositide species was sufficient, but for another 19, an additional signaling lipid was required (Figures 1A and S1O). This might explain why previous studies, based on the probing of single phosphoinositide species in vitro, often failed to detect efficient PH-domain recruitment to membranes (Yu et al., 2004). Comparing this data set to a set of 47 known, literature-derived, LBD-lipid interactions revealed a coverage of 68.1%. For instance, one of our false negatives is a missed interaction between OSH2 and PI(4)P (Table S4B) (Roy and Levine, 2004). Importantly, this coverage varied for the different PIP classes, reaching 86.7% for PI(4,5)P_2. To the best of our knowledge, the vast majority of the identified interactions have not been described previously. Among all PH domains included in our study, 34 have not been previously reported to interact with any membrane, and for an additional 26, we propose additional specificities and possible binding mechanisms (Table S4C). This includes interactions between a number of PH domains from nuclear proteins and specific phosphoinositide species known to regulate DNA-associated processes—such as nucleosome remodeling, transcription, and DNA replication—through poorly understood mechanisms (Tables S2 and S3) (Viiri et al., 2012; see below). The membrane-binding profiles of orthologous PH domain pairs correlated well (Pearson correlation = 0.63; p value < 2.2×10^{-16}), indicating that *C. thermophilum* domains have similar recruitment profiles as their counterpart in *S. cerevisiae* (Figure 1C). Because of the excellent biophysical properties of the proteome of this thermophilic fungus, the collection of *C. thermophilum* PH domains thus represents an ideal resource for follow-up structural and mechanistic studies (Amlacher et al., 2011). Overall, our approaches seem to be reliable and sensitive, and the data set contains important quantitative insights on the membrane-binding properties of PH domains.

Prevalence of Rheostasis: Driver versus Auxiliary Lipids

The quantitative binding profiling of such a large group of PH domains to a very diverse set of artificial membranes offers the opportunity to systematically explore some of the basic features that enable them to "read" specific membrane signatures, the so-called "phosphoinositide code" (Kutateladze, 2010). We first grouped the liposomes by scoring the similarity between pairs of PH-domain-binding profiles and used these scores for hierarchical clustering (see the Supplemental Experimental Procedures). The interaction profiles confirm that phosphoinositides are the preferred driver PH-domain ligands (Figures 2 and S2). Artificial membranes comprising more than one type of lipid and containing the same phosphoinositide species recruit similar sets of PH domains (Figure 2A). Remarkably though, the presence of additional, auxiliary lipids also plays a role—in particular, the lipid charge—and causes discrete but significant changes in the affinities of phosphoinositide-containing bilayers for some PH domains (Figure 2B).

To evaluate the role of cooperative associations or rheostasis (i.e., the changes in binding affinity for one lipid owing to the presence of another lipid) in the recruitment of PH domains to phosphoinositide-containing membranes, we derived a cooperativity index (CI = NBI_{L1+L2} / [NBI_{L1}+NBI_{L2}]). An interaction was considered cooperative when CI > 1, that is when the binding affinity to liposomes containing two signaling lipids was stronger than the sum of the binding affinities to liposomes containing the individual lipids. Simple additive interactions (NBI_{L1+L2} = NBI_{L1} + NBI_{L2}) were thus not considered. To account for technical variability, NBI_{L1+L2} also has to be higher than the highest value obtained for NBI_{L1}+NBI_{L2} among the replicates (Figures 3A, S3A, and S3B). Importantly, as the lipids were routinely analyzed at one concentration—which might already be saturating for some protein-liposome pairs—the data likely provide

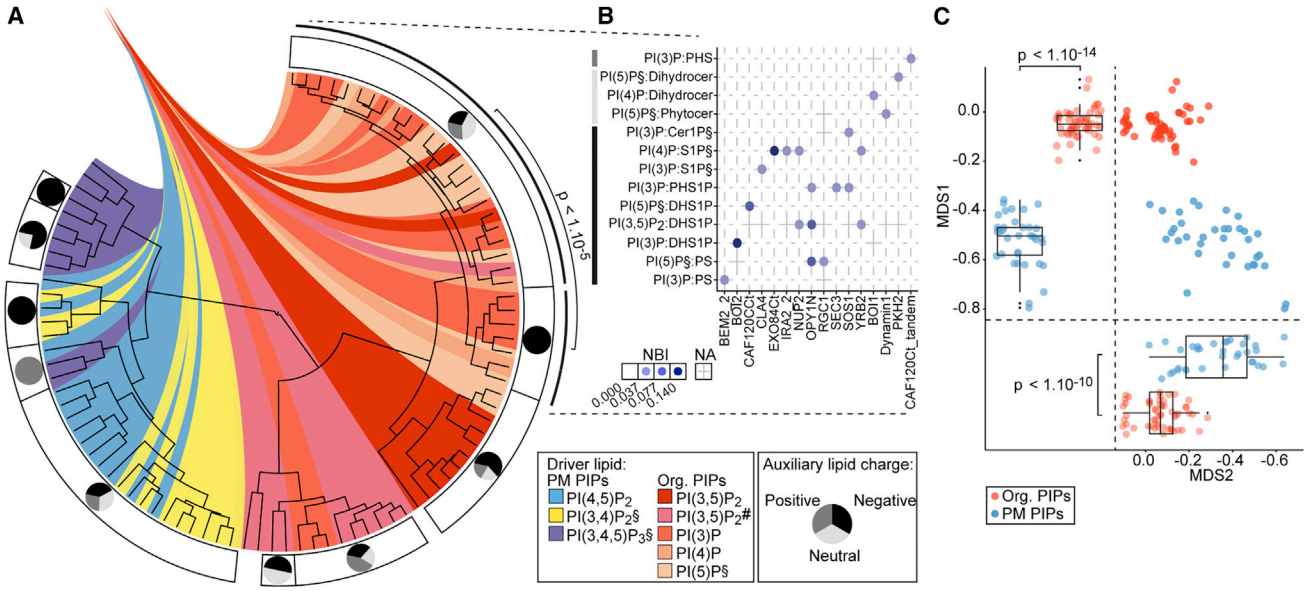

Figure 2. Clustering Analysis of Liposomes Based on Similarities in the Recruitment of PH Domains

(A) Hierarchical clustering of 90 liposome types composed of different combinations of phosphoinositides and an additional signaling lipid. Each liposome type is colored based on the phosphatidylinositol phosphate (PIP) species present in the mixture. The pie charts show the representation of charges of the auxiliary lipids within indicated subgroups, which correspond to depth of four from the root. # indicates an inactive (in our assay) dipalmitoyl variant of $PI(3,5)P_2$. The statistical significance was calculated on clades where the liposome types containing different PIP were randomly distributed (data not shown).

(B) Effect of the auxiliary lipid's charges on the PH domains-liposomes interactome within the clades highlighted in (A). Only interactions of PH domains that specifically interacted with liposomes containing auxiliary lipids of negative, positive, or neutral charge are shown.

(C) Principal coordinates analysis of PH-domain-binding profiles of all liposome types composed of combinations of signaling lipids. Red, liposomes containing organelle (Org) PIPs; blue, liposomes containing plasma membrane (PM) PIPs. MDS, multidimensional scaling; PI(3)P, early endosome; PI(4)P, Golgi, PM, late endosomes/lysosomes; $PI(3,5)P_2$, endosome/lysosome.

See also Figure S2.

a lower estimate for the fraction of cooperative binding events (see the high fraction of false negatives in Figure S3B, for which cooperativity was observed at lower lipid concentrations and that we marked with a star). We also observed instances of negative cooperativity ($NBI_{L1+L2} < \max\{NBI_{L1};NBI_{L2}\}$; $CI = NBI_{L1+L2}/\max\{NBI_{L1};NBI_{L2}\}$). However, they were very rare (33/247 = 13.4% of all cooperative events) and might give an estimate of our false-positive rate. Cooperative associations, implying phosphoinositide species and other auxiliary signaling lipids, were observed for the vast majority of the PH domains that bound liposomes (56/60; 93.3%). As a complementary approach, we performed detailed binding studies for 17 randomly selected cooperative interactions and could confirm 14 (82%); for the remaining three, the results were ambiguous (Figures 3B and S3B; protein concentrations are in Table S5B). The binding curves fit a model in which the binding intensity is proportional to the product of the two lipid concentrations, which is consistent with the view that the two lipids cooperate to efficiently recruit PH domains. Importantly, the dose-response experiments show that cooperativity also takes place when the concentration of $PI(4,5)P_2$ is lower than the one used for the initial screen (for example, YRB2, SWH1, and OPY1N; Figures 3B and S3B). Phosphorylated LCBs were the preferred phosphoinositide partners (Figure 3C). They contributed up to two times more frequently to cooperative interactions than other structurally related lipids (Figure 3D). Notably, signaling lipids that predominantly localize to the plasma membrane (PM), such as phosphatidylserine (PS) (Leventis and Grinstein, 2010) or ceramides (Schneiter et al., 1999), mostly partnered with phosphoinositide species also present at the PM—i.e., $PI(4,5)P_2$, $PI(3,4)P_2$, and $PI(3,4,5)P_3$ (Di Paolo and De Camilli, 2006) (Figure 3C). Overall, this indicates that these cooperative events are specific and apparently restricted to discrete pairs of signaling lipids.

Cooperative Mechanisms Fine-Tune the Recruitment of PH Domains to Biological Membranes In Vivo

The impact of coincidence sensing on the recruitment to artificial membrane is diverse (Figure 4A; Table S5C). For the 16 PH domains (out of the 54 implied in cooperative associations involving PIPs) that are selective for specific phosphoinositide species, the presence of auxiliary lipids caused significant changes in the phosphoinositide-binding specificity (Figure 4A, class 1). For instance, the PH domain of the kinase AKT1 strongly and specifically binds to liposomes containing either $PI(3,4,5)P_3$ or $PI(3,4)P_2$, yet the presence of LCBs induces a selective, ~5-fold increase in the affinity for $PI(4,5)P_2$ (Figures 4A and 4B), whereas the affinity to LCBs alone remains unchanged (data not shown). This is reminiscent of the behavior of an oncogenic form of AKT1 that carries an E17K mutation in its PH domain (Landgraf et al., 2008). When probed in our assay, this mutation triggers an increased affinity for $PI(4,5)P_2$ (Figure 4B) in vitro and constitutive targeting to the plasma membrane in vivo (Landgraf

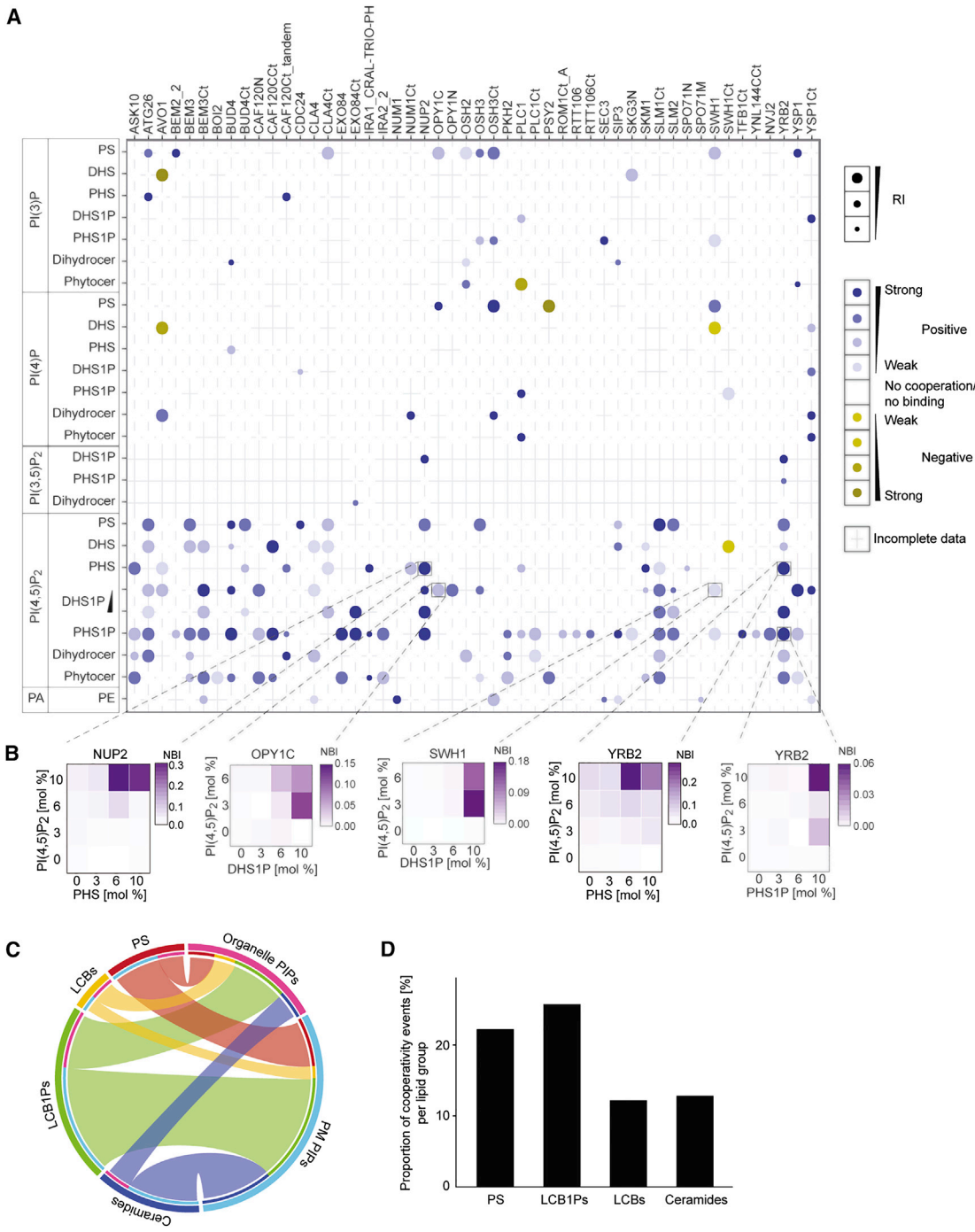

Figure 3. Landscape of Cooperating Lipids in the Targeting of Yeast PH Domains to Membranes

(A) Heatmap of cooperative indexes (CIs) calculated for PH domains (columns) and membranes containing combinations of physiological signaling lipids (rows; the wedge indicates low and high lipid concentrations, respectively). Only 50 PH domains with high-confidence CI > 1 for at least one liposome type are shown. RI: reproducibility index.

(B) Dose responses measured for the PH-domain interaction with liposomes containing the indicated concentration of signaling lipids. Values are means ($n \geq 2$).

(C) The summary of the propensity of different driver lipids (PIPs, right) and auxiliary lipids (left) to cooperate based on data shown in (A). Organelle PIPs and PM PIPs: as in Figure 2; ceramides: Cer, Cer1P, phytocer, and dihydrocer; LCB1Ps: S1P, DHS1P, and PHS1P; LCBs: sphingosine, DHS, and PHS.

(D) Cooperative interactions with regard to auxiliary lipids encountered. The bar plot gives the proportion of cooperative interactions of all experiments performed for each group of auxiliary lipids. LCB1Ps, LCBs, and ceramides are as in (C).

See also Figure S3.

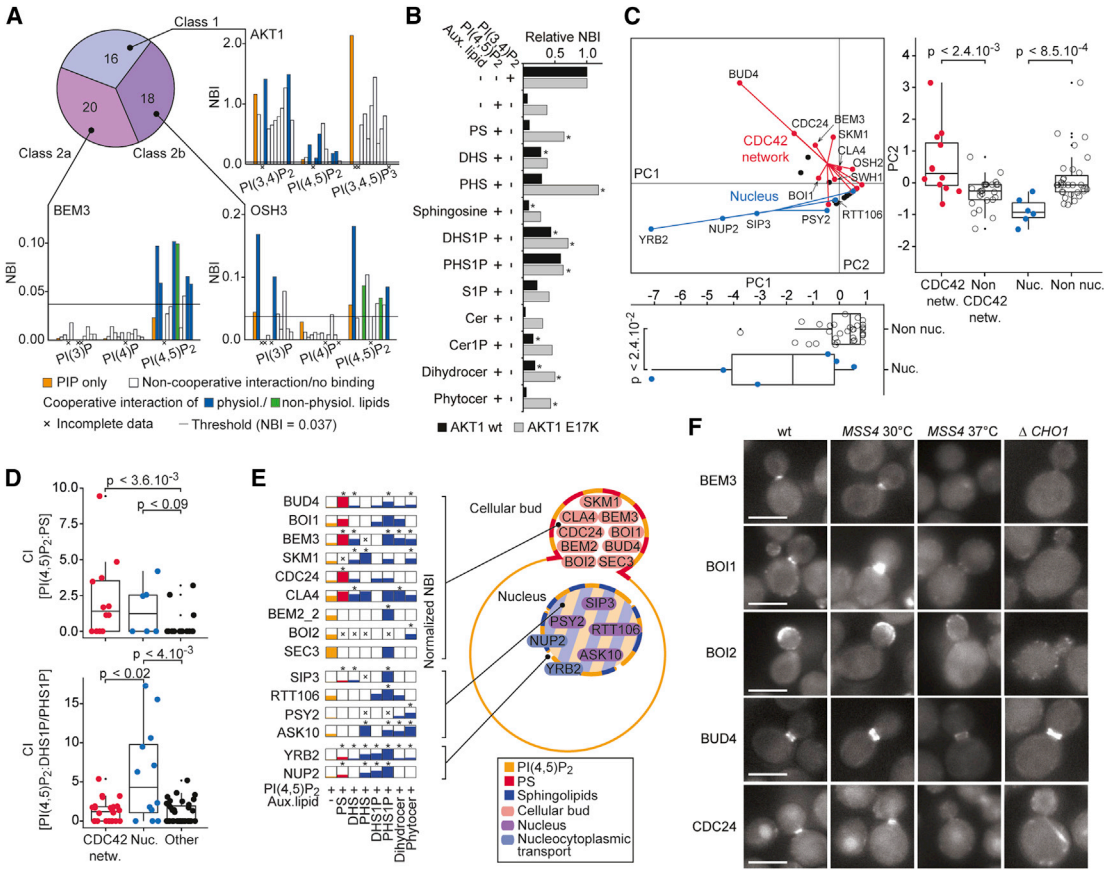

Figure 4. Cooperativity Fingerprints Reflect Protein Function and Localization

(A) Classification of different impacts of lipid cooperation on the membrane affinity of PH domains. The pie chart indicates the proportion of each class in our data set. The bar plots show the NBIs measured for liposomes containing PIPs alone or mixtures of PIPs with auxiliary lipids. The order of auxiliary lipids in the mixtures is (left to right) PS, DHS, PHS, sphingosine, DHS1P, PHS1P, S1P, Cer, Cer1P, dihydrocer, and phytocer.

(B) Influence of lipid cooperativity on membrane recruitment of AKT1-PH. Comparison of AKT1-PH wild-type (wt) and E17K NBIs to membranes of various lipid compositions. The NBI values for each AKT1 variant are normalized to the value of $PI(3,4)P_2$ only (relative NBI = 1). Stars indicate high-confidence cooperative interactions.

(C) Principal-component analysis of the *S. cerevisiae* PH domains with at least one CI > 1 (n = 37). Only CI values for liposomes containing $PI(4,5)P_2$ with PS/DHS1P/PHS1P were considered. The box plots represent the difference between nucleus and non-nucleus groups (bottom, PC1; right, PC2), and CDC42-interacting and non-interacting groups (right, PC2).

(D) Box plots of the CI values of $PI(4,5)P_2$:PS (top) or $PI(4,5)P_2$:DHS1P/PHS1P (bottom) liposomes calculated for the groups of PH domains defined in (C).

(E) Proteins targeted by the same cooperating lipid pairs are functionally related. Histograms show NBIs for $PI(4,5)P_2$ alone or in the presence of cooperating auxiliary lipids (CI > 1). Bars are normalized to the highest value for each individual PH domain. Stars indicate high-confidence cooperative interactions; crosses indicate incomplete data where the cooperativity could not be assessed.

(F) Impact of phosphatidylserine and $PI(4,5)P_2$ metabolism on the localization of selected GFP fusions in *S. cerevisiae*. Δ *CHO1*, phosphatidylserine synthase deletion; $MSS4^{ts}$, thermosensitive mutant of the phosphatidylinositol-4-phosphate 5-kinase. All scale bars represent 3 μm.

See also Figure S4.

et al., 2008). Notably, LCBs further increased the affinity of E17K AKT1 for $PI(4,5)P_2$ to levels that are similar to those observed for one of its physiological ligands $PI(3,4)P_2$, suggesting that cooperativity might also in part contribute to E17K AKT1-induced oncogenicity. For the remaining PH domains (38/54; 70.4%) that did not (20/54; 37.1%) or very poorly and non-specifically (18/54; 33.3%) bind to liposomes containing phosphoinositides alone (Yu et al., 2004), the presence of auxiliary lipids increased their affinity for specific phosphoinositide-containing liposomal membranes (Figure 4A, classes 2a and b; Table S5C). This might explain why previous studies, based on the probing of single phosphoinositide species in vitro, failed to detect efficient PH-domain recruitment to membranes (Yu et al., 2004). For example, the PH domain of BEM3—a membrane-associated GTPase-activating protein (GAP) for CDC42, a key regulator of polarized cell growth (Aguilar et al., 2006)—is known to poorly (if at all) bind artificial membranes containing only PIPs (Yu et al., 2004). However, it efficiently targets membranes that contain $PI(4,5)P_2$ and auxiliary signaling lipids; e.g., PS (see below).

To test the functional relevance of the identified cooperating lipid pairs (i.e., whether they contribute to a physiological membrane code), we related the in vitro binding profiles to

physiologically derived in vivo data. We first made use of annotations on protein-protein interactions and localization provided by STRING (Szklarczyk et al., 2011) and SGD (Nash et al., 2007), respectively. We observed that the proteins targeted by the same cooperating lipid pairs are functionally related and/or co-localize with their recruiting lipids (Figures 4C–4E). For instance, $PI(4,5)P_2$ and PS—two lipids that accumulate at the sites of polarized growth through mechanisms that imply vectorial delivery via secretory vesicles, active transport, and compartmentalized metabolism (Fairn et al., 2011)—most frequently cooperate to recruit PH domains from components of the CDC42 network that also generally localize at the budding sites (BEM2, BEM3, BOI1, BOI2, BUD4, CDC24, CLA4, OSH2, OSH3, SEC3, SKM1, and SWH1; Figures 4C–4E). The cooperativity between $PI(4,5)P_2$ and PS appear specific (Figure S4A). We also used live-cell imaging to determine the effect of perturbation of PS or $PI(4,5)P_2$ metabolism on the cellular localization of five proteins from the CDC42 network, BEM3, BOI1, BOI2, CDC24, and BUD4 fused to GFP (Figure 4F). We observed that both PS and $PI(4,5)P_2$ are required for their association with the sites of bud growth. This is consistent with the view that the two lipids might also cooperate in vivo. As controls, we also tested two proteins that localize at the bud neck but are not part of the CDC42 network, SKG3, and CAF120. The recruitment of SKG3 and CAF120 to both artificial membranes and yeast bud neck was unaffected by the absence of PS (Figure S4B).

Similarly, the PH domains present in nuclear proteins (ASK10, a component of RNA polymerase II; NUP2 and YRB2, involved in nucleocytoplasmic transport; PSY2, a DNA-damage checkpoint protein; RTT106, a histone chaperone; and SIP3, a transcription co-factor) are predominantly targeted by combinations of phosphoinositides and phosphorylated LCBs (e.g., DHS1P and/or PHS1P; Figures 4C–4E; Table S5C). This is consistent with recent evidence suggesting that a nuclear pool of these lipids plays a role in various nuclear functions (Lucki and Sewer, 2012; Viiri et al., 2012). Our data thus support the notion that cooperativity is a general and functionally relevant attribute of PH domains that frequently integrates affinity and specificity to expand the lipid code beyond the set of available phosphoinositides.

Targeting of PH Domains to Organelle and PM Phosphoinositides

Our data set indicates that the specificities of the PH domains encompass all seven phosphoinositide species (Figures 2A, S2A, and S2B) (Dowler et al., 2000). When grouping liposomes according to their PH-domain recruitment profiles, we observed that those containing phosphoinositides known to predominantly localize to the PM ($PI(4,5)P_2$, $PI(3,4)P_2$, and $PI(3,4,5)P_3$) and those containing other phosphoinositides also present in the organelles (PI(3)P, PI(4)P, PI(5)P, and $PI(3,5)P_2$; Hammond et al., 2014; van Meer et al., 2008) form two clusters that determine the propensity of the two types of membranes to recruit PH domains (Figures 2C, S2C, and S2D). By comparing the sequence of all PH domains that bind organelle phosphoinositides (OPs) with those that do not (Figure S5A), we derived a OP-binding consensus motif that comprises four residues located near the known lipid-binding site ($\beta1$-$\beta2$ loop and $\beta7$ strand) and five in other regions (e.g., a carboxy-terminal α helix; Figure 5A: OBM labeled in pink). The OP-binding consensus motif differs from the previously characterized BSM (Figure 5A; KXn(K/R)XR labeled in blue) that is present in all PH domains that bind phosphoinositides (Isakoff et al., 1998; Moravcevic et al., 2012; Park et al., 2008; Yu et al., 2004).

A Conserved, Organelle-Phosphoinositide-Binding Motif Is Perturbed in Some Cancer Biopsies

Next, we inspected the sequences of 1,205 PH domains annotated in the Uniprot database (UniProt Consortium, 2014) for the presence of this OP-binding motif (Figures 5B and S5B; Table S5A) and found that it is also conserved in higher eukaryotes, including humans. It is frequently—but not exclusively (see below)—present in the PH domains of lipid-transfer proteins that often associate with membrane contact sites specialized in specific lipid metabolism and signaling (Lev, 2010). This includes the PH domains of CERT, FAPP1, OSBP1, OSH2, and SWH1 that were known to bind OPs (Dowler et al., 2000; Levine and Munro, 2002; Roy and Levine, 2004). Importantly, the OP-binding motif is not restricted to lipid-transfer proteins, and 56% of the PH domains with the best OBM scores belong to other protein families (see Figures 5B and S5A; Table S5A). To validate the significance of the motif, we selected 13 PH domains (including ten from humans) for experimental confirmation (Figures 5B–5G; Table S5B). The selection also included four PH domains known to bind OPs (CERT, FAPP1, OSBP1, and SWH1) as controls (Dowler et al., 2000; Levine and Munro, 2002; Roy and Levine, 2004). The PH domains with a high OP-binding score (CERT, FAPP1, OPY1C, OSBP1, OSBP2, OSBPL3, OSPBL7, and SWH1) also mostly retain the basic sequence motif KXn(K/R)XR. These eight domains bound strongly to both organelle and PM phosphoinositides in vitro (Figure 5B), and the five domains we expressed in *S. cerevisiae* (CERT, FAPP1, OPY1C, OSBP2, and SWH1) co-localized with intracellular membrane structures, including some representing the Golgi (Figures 5C and 5G). By contrast, PH domains with the KXn(K/R)XR signature but with a largely incomplete OP-binding motif (OSBPL10, OSBPL11, and PLCD1) bound only weakly to OPs in vitro, whereas their affinities for PM phosphoinositides was high (Figures 5B and 5C). Finally, PH domains largely lacking both the OP-binding motif and the KXn(K/R)XR signature (OSBPL5 and OSBPL8) did not bind to any artificial membranes tested (Figure 5B).

We also introduced mutations to disrupt the OP-binding motif in four PH domains that bind OPs in vitro and in vivo (Figures 5D–5G and S5C; Table S5B). They were either artificially engineered (CERT-PH R98Q, FAPP1-PH K74Q, and SWH1-PH K360Q) or naturally observed in some human cancer biopsies (FAPP1-PH T9A and OSBP2-PH R262L; Imielinski et al., 2012; Network, 2012). For two domains, SWH1-PH K360Q and OSBP2-PH R262L, we also performed additional biophysical measurements using CD spectroscopy and confirmed that the two mutants were folded and stable under our experimental conditions (Figures S1B and S1C). In all cases, the mutations induced a very selective decrease in the affinity of the PH domain for OPs both in vitro and in vivo, whereas binding to PM phosphoinositides remained largely unaffected. This demonstrates that the OP-binding motif plays an important role in the proper subcellular localization of PH-domain-containing proteins, including families

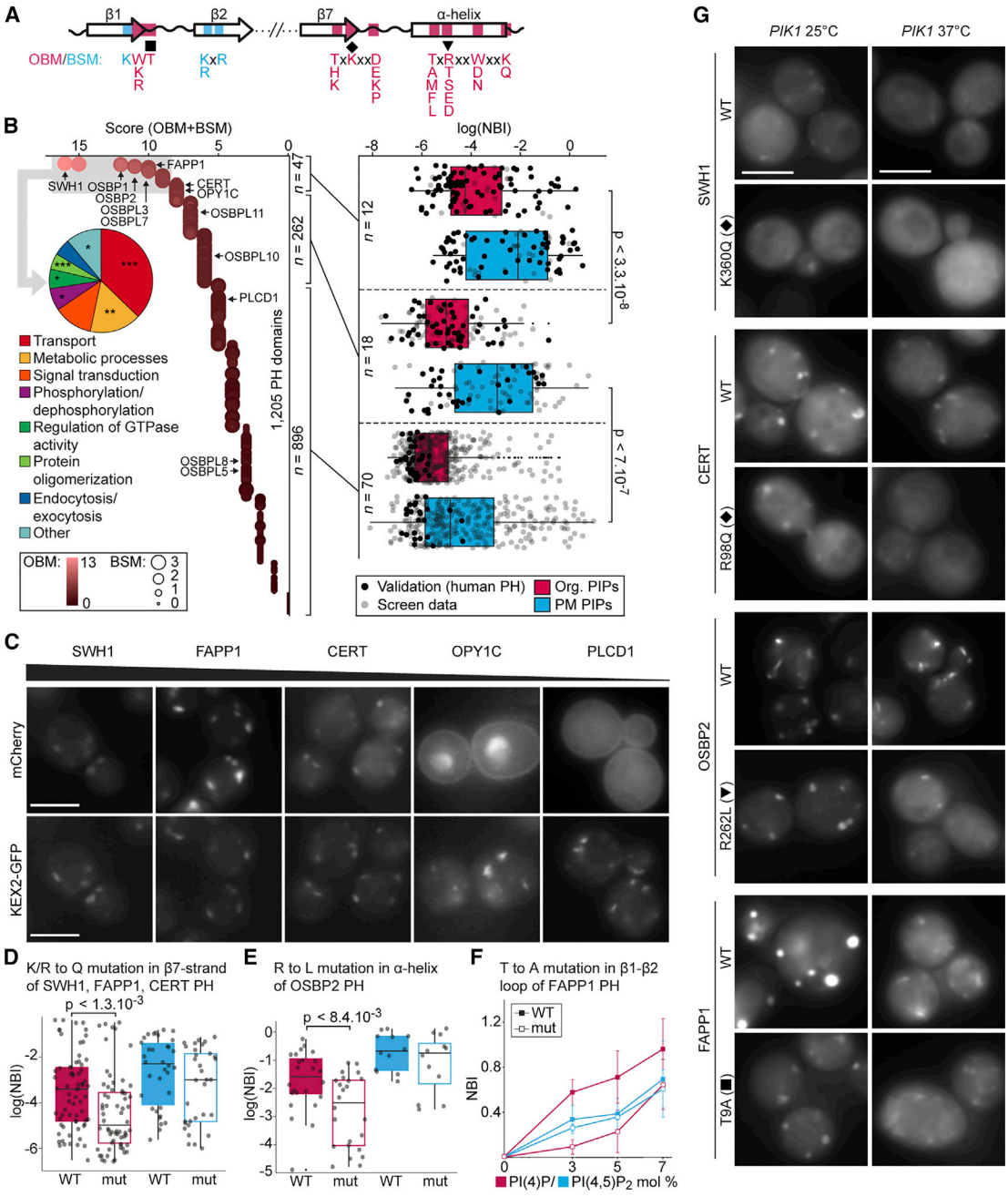

Figure 5. Characterization of a New Motif for Binding Organelle PIPs

(A) PH domain secondary structure representation with the positions of the organelle PIP-binding motif (OBM; pink) and basic sequence motif (BSM; blue).

(B) 1,205 PH domains are scored according to the OBM (color range) and BSM (circle size) conservation (left). The pie chart shows gene ontology annotations for the 47 highest-scoring PH domains. ***$p < 3.2 \times 10^{-12}$; **$p < 1.1 \times 10^{-6}$; *$p < 0.005$. The NBIs of 100 PH domains for either organelle PIPs (pink) or PM PIPs (blue) are shown (right).

(C) Intracellular localization of selected PH domains (mCherry-fusion) and trans-Golgi marker, KEX2 (GFP-fusion), in *S. cerevisiae*. The wedge indicates high and low OBM/BSM motif score.

(D and E) The NBIs measured for recruitment of WT and K/R to Q mutants of SWH1 (K360Q), FAPP1 (K74Q), and CERT PH (R98Q) domains (D) or WT and R262L mutant of OSBP2 PH domain (E) to liposomes containing organelle PIPs (pink) or PM PIPs (blue; n = 2).

(F) Dose-response recruitment of WT (filled squares) and T9A mutant (open squares) of FAPP1 PH domain to liposomes containing increasing concentrations of PI(4)P (pink) or $PI(4,5)P_2$ (blue; mean ± SD; n = 3).

(G) GFP fusions of selected WT and mutated PH domains expressed in a thermo-sensitive *PIK1^{ts} S. cerevisiae* strain.

All scale bars represent 3 μm. See also Figure S5.

of lipid-transfer proteins. Our data are also able to reveal the consequences of disease-associated mutations on the binding specificity of PH domains, which may contribute to current efforts in the design of small-molecule inhibitors of PH domains (Hussein et al., 2013).

DISCUSSION

Here, we report a large, systematic, and quantitative data set on the membrane-binding properties of PH domains, one of the most common domains in the human genome and mutations in which underlie several human diseases and syndromes. Our data reveal that the membrane recruitment of PH domains requires the presence of phosphoinositides but also that binding affinity and specificity are frequently determined by the presence of additional, auxiliary, signaling lipids that function as molecular rheostats. The most prominent among these are phosphorylated LCBs and PS, which are all conserved bioactive lipids with elusive mechanisms of actions. They are known to be targeted by only a small number of domains, suggesting that rheostasis might represent their primary, fundamental signaling mode. LCBs and PS, like many other lipids, are heterogeneously distributed within cellular and organelle membranes, and this compartmentalization—implying spatially regulated metabolism, lateral lipid segregation, and active lipid transport—may contribute to the generation of the coincidence signals. Coincidence sensing might work via the presence of a lipid-binding pocket containing two binding sites. Structural and biophysical studies of some prototypic PH domains suggest the presence of additional positively charged binding sites for anionic, auxiliary lipids (Gallego et al., 2010). Otherwise, we can speculate that the auxiliary lipids induce local reorganization of the membrane and the formation of nanoscale PIP-containing lipid domains (van den Bogaart et al., 2011). The emergence of a class of synthetic lipids with a caged head group (Höglinger et al., 2014) will allow to further discriminate between these mechanisms. The frequency of cooperativity and the apparent diversity of the auxiliary lipids involved all point to the importance of such events. These basic membrane recruitment principles, which might also hold for other LBDs (Gallego et al., 2010), may contribute to the spatiotemporal tuning of signaling and thus expand the lipid code beyond the set of available phosphoinositides.

Finally, our study can be considered as a proof of principle for the feasibility of comprehensive and systematic analyses of protein recruitment to membranes and indicates that our quantitative screening approach (Saliba et al., 2014) is scalable to entire proteomes and lipidomes.

EXPERIMENTAL PROCEDURES

LBDs Expression and Preparation of Cell Extracts

The lipid-binding domains (LBDs) were expressed as N-terminal His6-SUMO3 and C-terminal sfGFP (Pédelacq et al., 2006) fusions in *E. coli* (BL21 STAR; Invitrogen; see Table S5D for sequences of primers). Cell lysis was performed as described previously (Saliba et al., 2014).

LiMA Experimental Procedure

The fabrication of liposome microarrays, the experimental procedure of protein-liposome interaction assay, the image analysis, and the calculation of normalized binding intensity (NBI) values were described previously (Saliba et al., 2014). Briefly, liposomes were formed in a buffer with a physiological salt concentration (150 mM NaCl) from lipid mixtures containing various combinations of 26 signaling lipids (Table S1). The liposomes were incubated 20 min in the cell extracts containing sfGFP-tagged proteins. Subsequently, the unbound material was washed and the interactions were monitored by automated microscopy. Fluorescence intensities from pixels matching liposomal membranes were extracted and used for calculation of NBIs.

The details of the selection of LBDs, the protocol for the production of recombinant proteins, the detailed composition of all liposome microarrays used, the preparation and imaging of yeast strains, and the computational data analysis are described in the Supplemental Experimental Procedures.

SUPPLEMENTAL INFORMATION

Supplemental Information includes Supplemental Experimental Procedures, five figures, and five tables and can be found with this article online at http://dx.doi.org/10.1016/j.celrep.2015.07.054.

AUTHOR CONTRIBUTIONS

I.V., A.-E.S., P.B., and A.-C.G. designed the research with the expert help of J.E.; I.V., A.-E.S., S.D., S.C., A.G., K.G.K., and V.v.N. conducted the experiments and performed the analysis; I.V. and A.-E.S. did almost all of the experimental work and S.D. did almost all of the bioinformatic analyses presented here; K.M. and V.R. contributed to the biochemical and biophysical protocols; K.A. and T.D. performed the PH-domain prediction; and I.V., A.-E.S., S.D., P.B., and A.-C.G. discussed results and wrote the manuscript with support from all the authors.

ACKNOWLEDGMENTS

We are grateful to E. Hurt and M. Kaksonen for inspiring comments on the manuscript and to the EMBL Advanced Light Microscopy and the Protein Expression and Purification Core Facilities, G. Zeller, C. Tischer, C. Besir, M.M. Hemberger, and C. Merten for expert help and the sharing of reagents. We thank N. Silva Martin (EMBL) for cDNA from *C. thermophilum*, J. Holthuis (University of Osnabrück) for providing HA-CERT-pcDNA3.1 plasmid, E.C. Hurt (BZH, Heidelberg University) for pRS315-mCherry vector, and S. Emr (Weill Institute for Cell and Molecular Biology, Cornell University) for *pik1*^{ts} strain. We thank Y.P. Yuan for providing Information Technology infrastructure. We also thank other members of P.B.'s, J.E.'s, and A.-C.G.'s groups for continuous discussions and support. This work is partially funded by the DFG in the framework of the Cluster of Excellence, CellNetworks Initiative of the University of Heidelberg (ExIni, EcTop) to K.M. A.-E.S. is supported by the European Molecular Biology Laboratory and the EU Marie Curie Actions Interdisciplinary Postdoctoral Cofunded Programme. K.A. thankfully acknowledges support from Marie Curie reintegration grant (ERG). Funding for open access charge was supported by the European Molecular Biology Laboratory. The authors declare competing financial interests in the form of a patent application based on the methods, LiMA, used for this work.

Received: July 28, 2014
Revised: June 30, 2015
Accepted: July 27, 2015
Published: August 20, 2015

REFERENCES

Aguilar, R.C., Longhi, S.A., Shaw, J.D., Yeh, L.Y., Kim, S., Schön, A., Freire, E., Hsu, A., McCormick, W.K., Watson, H.A., and Wendland, B. (2006). Epsin N-terminal homology domains perform an essential function regulating Cdc42 through binding Cdc42 GTPase-activating proteins. Proc. Natl. Acad. Sci. USA *103*, 4116–4121.

Amlacher, S., Sarges, P., Flemming, D., van Noort, V., Kunze, R., Devos, D.P., Arumugam, M., Bork, P., and Hurt, E. (2011). Insight into structure and

assembly of the nuclear pore complex by utilizing the genome of a eukaryotic thermophile. Cell *146*, 277–289.

Anand, K., Maeda, K., and Gavin, A.C. (2012). Structural analyses of the Slm1-PH domain demonstrate ligand binding in the non-canonical site. PLoS ONE *7*, e36526.

Bayascas, J.R., Wullschleger, S., Sakamoto, K., García-Martínez, J.M., Clacher, C., Komander, D., van Aalten, D.M., Boini, K.M., Lang, F., Lipina, C., et al. (2008). Mutation of the PDK1 PH domain inhibits protein kinase B/Akt, leading to small size and insulin resistance. Mol. Cell. Biol. *28*, 3258–3272.

Burger, K.N., Demel, R.A., Schmid, S.L., and de Kruijff, B. (2000). Dynamin is membrane-active: lipid insertion is induced by phosphoinositides and phosphatidic acid. Biochemistry *39*, 12485–12493.

Di Paolo, G., and De Camilli, P. (2006). Phosphoinositides in cell regulation and membrane dynamics. Nature *443*, 651–657.

Dowler, S., Currie, R.A., Campbell, D.G., Deak, M., Kular, G., Downes, C.P., and Alessi, D.R. (2000). Identification of pleckstrin-homology-domain-containing proteins with novel phosphoinositide-binding specificities. Biochem. J. *351*, 19–31.

Fairn, G.D., Hermansson, M., Somerharju, P., and Grinstein, S. (2011). Phosphatidylserine is polarized and required for proper Cdc42 localization and for development of cell polarity. Nat. Cell Biol. *13*, 1424–1430.

Gallego, O., Betts, M.J., Gvozdenovic-Jeremic, J., Maeda, K., Matetzki, C., Aguilar-Gurrieri, C., Beltran-Alvarez, P., Bonn, S., Fernández-Tornero, C., Jensen, L.J., et al. (2010). A systematic screen for protein-lipid interactions in Saccharomyces cerevisiae. Mol. Syst. Biol. *6*, 430.

Hammond, G.R., Machner, M.P., and Balla, T. (2014). A novel probe for phosphatidylinositol 4-phosphate reveals multiple pools beyond the Golgi. J. Cell Biol. *205*, 113–126.

Höglinger, D., Nadler, A., and Schultz, C. (2014). Caged lipids as tools for investigating cellular signaling. Biochim. Biophys. Acta *1841*, 1085–1096.

Huang, B.X., Akbar, M., Kevala, K., and Kim, H.Y. (2011). Phosphatidylserine is a critical modulator for Akt activation. J. Cell Biol. *192*, 979–992.

Huh, W.K., Falvo, J.V., Gerke, L.C., Carroll, A.S., Howson, R.W., Weissman, J.S., and O'Shea, E.K. (2003). Global analysis of protein localization in budding yeast. Nature *425*, 686–691.

Hussein, M., Bettio, M., Schmitz, A., Hannam, J.S., Theis, J., Mayer, G., Dosa, S., Gütschow, M., and Famulok, M. (2013). Cyplecksins are covalent inhibitors of the pleckstrin homology domain of cytohesin. Angew. Chem. Int. Ed. Engl. *52*, 9529–9533.

Imielinski, M., Berger, A.H., Hammerman, P.S., Hernandez, B., Pugh, T.J., Hodis, E., Cho, J., Suh, J., Capelletti, M., Sivachenko, A., et al. (2012). Mapping the hallmarks of lung adenocarcinoma with massively parallel sequencing. Cell *150*, 1107–1120.

Isakoff, S.J., Cardozo, T., Andreev, J., Li, Z., Ferguson, K.M., Abagyan, R., Lemmon, M.A., Aronheim, A., and Skolnik, E.Y. (1998). Identification and analysis of PH domain-containing targets of phosphatidylinositol 3-kinase using a novel in vivo assay in yeast. EMBO J. *17*, 5374–5387.

Knight, J.D., and Falke, J.J. (2009). Single-molecule fluorescence studies of a PH domain: new insights into the membrane docking reaction. Biophys. J. *96*, 566–582.

Köberlin, M.S., Snijder, B., Heinz, L.X., Baumann, C.L., Fauster, A., Vladimer, G.I., Gavin, A.-C., and Superti-Furga, G. (2015). A conserved circular network of coregulated lipids modulates innate immune responses. Cell *162*, 170–183.

Kutateladze, T.G. (2010). Translation of the phosphoinositide code by PI effectors. Nat. Chem. Biol. *6*, 507–513.

Kutateladze, T.G., Capelluto, D.G., Ferguson, C.G., Cheever, M.L., Kutateladze, A.G., Prestwich, G.D., and Overduin, M. (2004). Multivalent mechanism of membrane insertion by the FYVE domain. J. Biol. Chem. *279*, 3050–3057.

Landgraf, K.E., Pilling, C., and Falke, J.J. (2008). Molecular mechanism of an oncogenic mutation that alters membrane targeting: Glu17Lys modifies the PIP lipid specificity of the AKT1 PH domain. Biochemistry *47*, 12260–12269.

Lee, M.H., and Bell, R.M. (1991). Mechanism of protein kinase C activation by phosphatidylinositol 4,5-bisphosphate. Biochemistry *30*, 1041–1049.

Lemmon, M.A. (2003). Phosphoinositide recognition domains. Traffic *4*, 201–213.

Lemmon, M.A. (2008). Membrane recognition by phospholipid-binding domains. Nat. Rev. Mol. Cell Biol. *9*, 99–111.

Lev, S. (2010). Non-vesicular lipid transport by lipid-transfer proteins and beyond. Nat. Rev. Mol. Cell Biol. *11*, 739–750.

Leventis, P.A., and Grinstein, S. (2010). The distribution and function of phosphatidylserine in cellular membranes. Annu. Rev. Biophys. *39*, 407–427.

Levine, T.P., and Munro, S. (2002). Targeting of Golgi-specific pleckstrin homology domains involves both PtdIns 4-kinase-dependent and -independent components. Curr. Biol. *12*, 695–704.

Lindhurst, M.J., Sapp, J.C., Teer, J.K., Johnston, J.J., Finn, E.M., Peters, K., Turner, J., Cannons, J.L., Bick, D., Blakemore, L., et al. (2011). A mosaic activating mutation in AKT1 associated with the Proteus syndrome. N. Engl. J. Med. *365*, 611–619.

Lucas, N., and Cho, W. (2011). Phosphatidylserine binding is essential for plasma membrane recruitment and signaling function of 3-phosphoinositide-dependent kinase-1. J. Biol. Chem. *286*, 41265–41272.

Lucki, N.C., and Sewer, M.B. (2012). Nuclear sphingolipid metabolism. Annu. Rev. Physiol. *74*, 131–151.

Macia, E., Paris, S., and Chabre, M. (2000). Binding of the PH and polybasic C-terminal domains of ARNO to phosphoinositides and to acidic lipids. Biochemistry *39*, 5893–5901.

Mitra, P., Zhang, Y., Rameh, L.E., Ivshina, M.P., McCollum, D., Nunnari, J.J., Hendricks, G.M., Kerr, M.L., Field, S.J., Cantley, L.C., and Ross, A.H. (2004). A novel phosphatidylinositol(3,4,5)P3 pathway in fission yeast. J. Cell Biol. *166*, 205–211.

Moravcevic, K., Oxley, C.L., and Lemmon, M.A. (2012). Conditional peripheral membrane proteins: facing up to limited specificity. Structure *20*, 15–27.

Nash, R., Weng, S., Hitz, B., Balakrishnan, R., Christie, K.R., Costanzo, M.C., Dwight, S.S., Engel, S.R., Fisk, D.G., Hirschman, J.E., et al. (2007). Expanded protein information at SGD: new pages and proteome browser. Nucleic Acids Res. *35*, D468–D471.

Network, C.G.A.; Cancer Genome Atlas Network (2012). Comprehensive molecular characterization of human colon and rectal cancer. Nature *487*, 330–337.

Park, W.S., Heo, W.D., Whalen, J.H., O'Rourke, N.A., Bryan, H.M., Meyer, T., and Teruel, M.N. (2008). Comprehensive identification of PIP3-regulated PH domains from C. elegans to H. sapiens by model prediction and live imaging. Mol. Cell *30*, 381–392.

Pédelacq, J.D., Cabantous, S., Tran, T., Terwilliger, T.C., and Waldo, G.S. (2006). Engineering and characterization of a superfolder green fluorescent protein. Nat. Biotechnol. *24*, 79–88.

Roy, A., and Levine, T.P. (2004). Multiple pools of phosphatidylinositol 4-phosphate detected using the pleckstrin homology domain of Osh2p. J. Biol. Chem. *279*, 44683–44689.

Saliba, A.E., Vonkova, I., Ceschia, S., Findlay, G.M., Maeda, K., Tischer, C., Deghou, S., van Noort, V., Bork, P., Pawson, T., et al. (2014). A quantitative liposome microarray to systematically characterize protein-lipid interactions. Nat. Methods *11*, 47–50.

Schneiter, R., Brügger, B., Sandhoff, R., Zellnig, G., Leber, A., Lampl, M., Athenstaedt, K., Hrastnik, C., Eder, S., Daum, G., et al. (1999). Electrospray ionization tandem mass spectrometry (ESI-MS/MS) analysis of the lipid molecular species composition of yeast subcellular membranes reveals acyl chain-based sorting/remodeling of distinct molecular species en route to the plasma membrane. J. Cell Biol. *146*, 741–754.

Stahelin, R.V., Burian, A., Bruzik, K.S., Murray, D., and Cho, W. (2003). Membrane binding mechanisms of the PX domains of NADPH oxidase p40phox and p47phox. J. Biol. Chem. *278*, 14469–14479.

Stahelin, R.V., Ananthanarayanan, B., Blatner, N.R., Singh, S., Bruzik, K.S., Murray, D., and Cho, W. (2004). Mechanism of membrane binding of the phospholipase D1 PX domain. J. Biol. Chem. *279*, 54918–54926.

Szklarczyk, D., Franceschini, A., Kuhn, M., Simonovic, M., Roth, A., Minguez, P., Doerks, T., Stark, M., Muller, J., Bork, P., et al. (2011). The STRING database in 2011: functional interaction networks of proteins, globally integrated and scored. Nucleic Acids Res. *39*, D561–D568.

Trajkovic, K., Hsu, C., Chiantia, S., Rajendran, L., Wenzel, D., Wieland, F., Schwille, P., Brügger, B., and Simons, M. (2008). Ceramide triggers budding of exosome vesicles into multivesicular endosomes. Science *319*, 1244–1247.

UniProt Consortium (2014). Activities at the Universal Protein Resource (UniProt). Nucleic Acids Res. *42*, D191–D198.

van den Bogaart, G., Meyenberg, K., Risselada, H.J., Amin, H., Willig, K.I., Hubrich, B.E., Dier, M., Hell, S.W., Grubmüller, H., Diederichsen, U., and Jahn, R. (2011). Membrane protein sequestering by ionic protein-lipid interactions. Nature *479*, 552–555.

van Meer, G. (2005). Cellular lipidomics. EMBO J. *24*, 3159–3165.

van Meer, G., Voelker, D.R., and Feigenson, G.W. (2008). Membrane lipids: where they are and how they behave. Nat. Rev. Mol. Cell Biol. *9*, 112–124.

Viiri, K., Mäki, M., and Lohi, O. (2012). Phosphoinositides as regulators of protein-chromatin interactions. Sci. Signal. *5*, pe19.

Yu, J.W., and Lemmon, M.A. (2001). All phox homology (PX) domains from Saccharomyces cerevisiae specifically recognize phosphatidylinositol 3-phosphate. J. Biol. Chem. *276*, 44179–44184.

Yu, J.W., Mendrola, J.M., Audhya, A., Singh, S., Keleti, D., DeWald, D.B., Murray, D., Emr, S.D., and Lemmon, M.A. (2004). Genome-wide analysis of membrane targeting by S. cerevisiae pleckstrin homology domains. Mol. Cell *13*, 677–688.

Ziemba, B.P., and Falke, J.J. (2013). Lateral diffusion of peripheral membrane proteins on supported lipid bilayers is controlled by the additive frictional drags of (1) bound lipids and (2) protein domains penetrating into the bilayer hydrocarbon core. Chem. Phys. Lipids *172-173*, 67–77.

Züchner, S., Noureddine, M., Kennerson, M., Verhoeven, K., Claeys, K., De Jonghe, P., Merory, J., Oliveira, S.A., Speer, M.C., Stenger, J.E., et al. (2005). Mutations in the pleckstrin homology domain of dynamin 2 cause dominant intermediate Charcot-Marie-Tooth disease. Nat. Genet. *37*, 289–294.